8 Application of the two-layer gauges on tip leakage flows

8.1 Introduction

The leakage flow across the blade tip of unshrouded rotors increases the stage losses and generates high heat transfer coefficients at the near tip regions resulting in loss of material and/or erosion that produce even higher losses. Intensive flow studies are required in order to reduce these undesirable effects of the leakage flow and/or to introduce new tip leakage sealing treatments. There already exists a large amount of literature that examines different blade tip geometries under different operating conditions and tries to describe more into detail the flow across the blade tip (see appendix 18.7). At VKI, heat transfer measurements on flat and squealer blade tips are performed with the two-layer gauges technique and the results are described in the following chapters.

8.2 Description of the tip leakage flows

During the turbine operation, the rotation of the rotor, which is enclosed in the stationary casing, requires a small gap between the rotor tip and the inside casing, called tip clearance. Despite the small size of this gap (around *1* to *3%* of the rotor blade span), the pressure difference between the suction and the pressure side of the blade near the tip region drives a flow across the blade tip called tip leakage flow.

The magnitude of the tip clearance during the turbine operation varies as the latter operates in a transient regime. Different thermal expansions between the rotor and the casing result in different thermal displacements of the rotor compared to the stator, influencing the tip clearance. Figure 8-1 that presents a typical engine operational chart (rotor speed variation and corresponding rotor and casing growth/contraction) is published by Glezer (2004). The rotor engine thermal response (ΔR rotor) is slower than the casing (ΔR stator) which is favorable when the engine starts. However, after an emergency shut down from steady state operation, the tip clearance is suddenly reduced and can eventually be closed resulting in potential rub of the rotor on the casing. Exactly at that moment, the engine should be restarted to avoid the rub. Thus, the control of the tip clearance is of great importance as its magnitude significantly changes during the turbine operation.

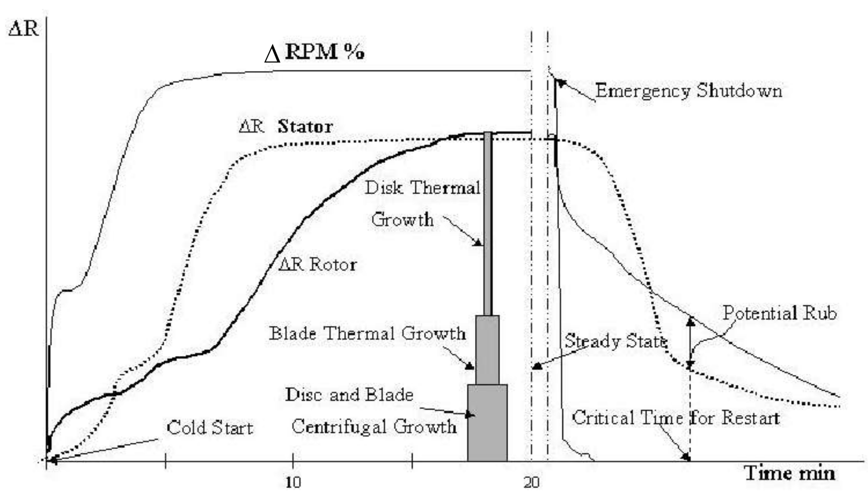

Figure 8-1: Typical transient rotor and stator (casing) radial growth (Glezer, 2004)

The tip leakage flow that passes almost axially across the blade tip without being really turned reduces the possible extraction of work by off-loading the blade tip region and thus deteriorates the aerodynamic performance of the turbine stage. In addition, the tip leakage flow also mixes with the oncoming flow on the suction side of the blade near the tip and thus increases the flow entropy. To sum up the two previous statements, the tip clearance losses represent a large component of the overall loss in a turbine with an unshrouded rotor. Figure 8-2 is taken from Booth (1985), the data originally being from Boyle et al. (1984), and represents the loss breakdown for a number of early shroudless high pressure research turbines. (Each horizontal line in the figure separates the different loss contributions for every turbine as a percentage of the total loss.) Even with larger turbines such as 42A, the tip clearance loss represents *25%* of the total loss in the whole stage that is about one third of the rotor loss.

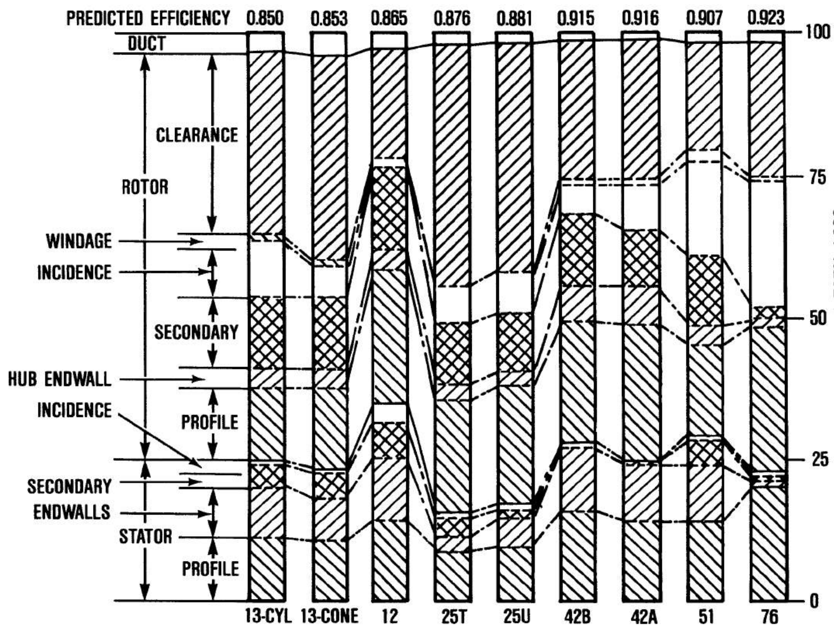

Figure 8-2: Sources of loss in nine different turbine stages (from 13-CYL till 76) (Booth, 1985)

The continuous demand on increasing the cycle efficiencies of the turbines results in continuously increasing turbine inlet temperatures and thus in higher tip leakage flow temperatures across the blade tips. Figure 8-3 is taken from Ameri (2004), the data originally being from Dr. T. Yoshida, Japan, and shows this trend clearly for both aero and industrial engines. The high temperature tip leakage flow highly accelerates across the blade tip generating very thin boundary layers and creates high heat transfer coefficients and non-uniformities on the blade tip and near tip regions. As a result, high thermal stresses are produced; because they are combined with the high mechanical stresses (because of the furthest radial position of the blade at the tip), they cause tip burnout, erosion, oxidation, thermal fatigue and creep. Then the tip clearance widens and the losses increase even more. The blade tip region is the most frequently inspected and repaired area due to frequent breakdowns.

In general, the tip leakage flow and the heat transfer on the blade tip and near tip region are very complex, three-dimensional, and unsteady. The understanding of this flow helps to control the tip clearance in a better way and to introduce new tip leakage sealing mechanisms so that the undesirable effects are reduced. Tighter clearance gaps let less mass (leakage) flow to pass and increase the efficiency of the stage. Although the internal or film cooling schemes are difficult to be situated at the tip, they can protect the tip region from the hot gases that the blade is exposed from all sides. Recessed tip blades such as squealers act as a labyrinth seal increasing the resistance to the tip leakage flow. They can also operate in smaller clearances without the risk of catastrophic failure in case of rubs against the casing. The latest years, also shrouded rotor blade tips are developed that highly diminish the leakage flow. However, the weight of the shrouded rotor increases (compared to the unshrouded one) reducing the work extraction.

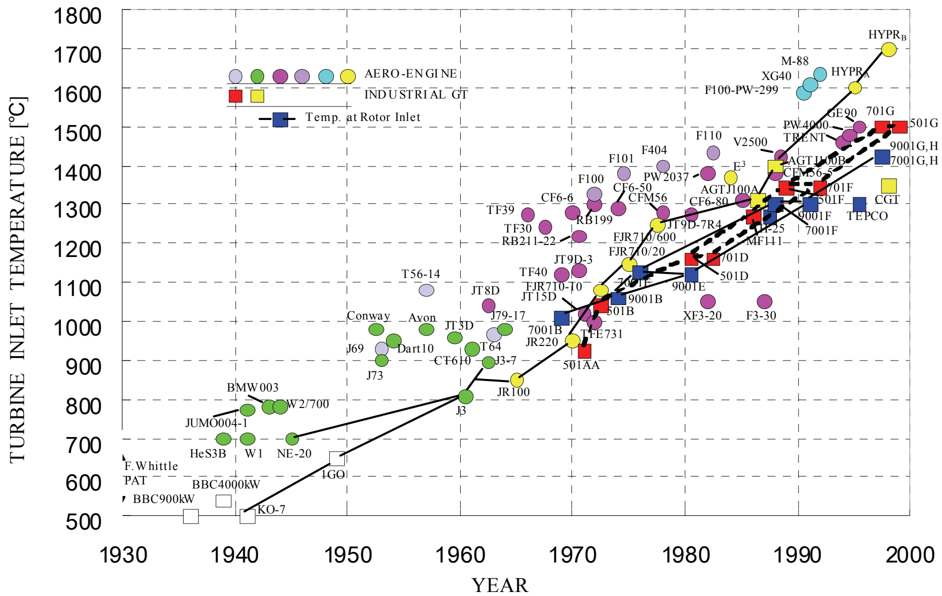

Figure 8-3: The upward trend in turbine inlet temperature (Ameri, 2004)

8.3 Necessity of the measurements on the VKI rotor blade tip

At VKI, heat transfer measurements on flat and squealer blade tips are performed with the two-layer gauges technique. The flat tip geometry is similar to the rotor blade tip that is used in the one and a half stage turbine of the VKI Isentropic Light Piston facility, CT3. The measurements were performed on a four bladed linear cascade in the VKI Isentropic Light Piston facility, CT2. Earlier determination of the leakage flow across the blade tip was performed by Key and Arts (2004) through flow visualizations and static pressure measurements on the tip and near tip regions. The heat transfer measurements come to complete the flow study and to quantify the thermal effects on the blade tip.

In the literature, earlier heat transfer measurements and predictions have been achieved on different blade tip geometries than the one used at VKI (see appendix 18.7). However, the tip leakage flow depends on the blade tip geometry and the loading near the tip. The need of examining each tip geometry separately arises, when thorough knowledge of the flow is necessary.

Only few measurements were performed in the past in high speed flows with cascades or turbines, thus, this VKI study that simulates high exit Reynolds numbers and high exit Mach numbers, comparable to the ones used in real engines (Table 8-3), offers more information about the leakage flow behavior in real engine environments. Emphasis is also given on the influence of the free stream turbulence intensity, as well as on the influence of thick inlet boundary layers on the tip heat transfer. Both parameters are close to the real engine conditions.

The heat transfer measurements at VKI were performed under hot free stream flow (*340K*), contrary to most of the earliest measurements in cascades. Only a couple of measurements in real rotors used hot free stream flow in the past, but then the spatial resolution of the gauges was not as high as the one in VKI measurements. The size of the blades in the VKI cascade is scaled up and thus the number of the gauges over the tip is increased. No additional preliminary heating of the blades (that generate natural convection losses) is needed and the heat flux comes from the flow on the blade surface.

The choice of the two-layer gauges technique to measure the wall heat flux on two VKI rotor blade tips (flat and squealer geometry) is of primary importance. This technique is already well studied and validated at 50% span of the second stator blade of the one and a half stage turbine of the CT3 facility (chapter 5). The gauges can be easily glued on any flat geometry such as the blade tips without any additional machining or cutting of the blade tips (contrary to the single-layer Macor gauges (chapter 4)); they do not disturb the flow development over the tip that is highly complicated in a very small space (contrary to the thermocouples); they do not need any transparent enwall window (contrary to liquid crystals); they operate with hot free stream flow, while being initially at ambient temperature without the need of heating (contrary to liquid crystals); they are much faster response than the liquid crystals and operate transiently in the VKI short duration facilities, CT2 and CT3, allowing several different tests per day. Moreover, the successful application of the gauges in a highly complicated flow such as the tip leakage flow (that consists of flow impingement areas, recirculation, vortices, transitional boundary layers etc) clearly demonstrates the advantages of the new developed technique.

8.4 Design and application of the two-layer gauges on the blade tip

The following paragraphs describe the application of the two-layer gauges on two tip geometries: flat tip and squealer tip. Both blade tip geometries were suggested by the European research project: 'Aerothermal Investigation of Turbine Enwalls and Blade' (AITEB, 5FP, G4RD-CT-1999-00055). The flat tip is also similar to the rotor blade tip that is used in the one and a half stage turbine of the CT3 facility, but scaled up *2.5* times. The bigger size of the blades allows more sensors on the blade tip and increases the spatial resolution of the measurements. The scaled up factor *2.5* is chosen to fit the four bladed linear cascade in the test section of the VKI CT2 facility.

The thin film resistances are deposited on a $50\ \mu m$ Upilex-S sheet, which is then glued on the blade tips by a two-sided $75\ \mu m$ adhesive sheet. The Upilex-S and the adhesive are bought from TAO SYSTEMS (USA) and the assembly is carried out at VKI. The $125\ \mu m$ thickness of the gauges is taken into account while the blade is machined, so that the total tip gap clearance (between the gauges and the enwall) is *1.325 mm* for the flat tip (left sketch of Figure 8-4). Gauges are also instrumented on the cavity of the squealer blade tip geometry; there are no gauges on the squealer rim. The total squealer groove height (from the gauges till the top of the squealer rim) is *2.65 mm*, while the blade groove height is $125\ \mu m$ bigger. The tip clearance between the squealer rim and the enwall is kept *1.325 mm* equal to one of the flat tip (right sketch of Figure 8-4). The flat blade tip or the cavity profile for the two tip geometries is already provided on the Upilex-S sheets by the company. The design of the two Upilex-S sheets together with the thin film resistances their corresponding numbering (from -3 to 8 for flat tip and -3 to 7 for squealer tip) and their connections are shown in Figure 8-5. The connections of the gauges (shown with two different colors for each gauge, so that they can be better distinguished) were transferred all together at two places at the suction side of the blade tip; the main objective is to eliminate the chances of disturbing the flow across and on the blade tip, thus, the connections are chosen to be transferred at the blade side where the leakage flow leaves the gap (suction side) instead of the pressure side. More specifically, two additional very thin flat grooves are machined at the blades suction sides and the connections were transferred through them till the bottom of the blades. Then, these grooves are covered with a two component adhesive (UHU plus). This material is first in a liquid form, best for covering all the holes and then gets solid. It is also easily machinable and the final profile of the suction side of the blade can be restored in a fast and accurate way. The joint of UHU plus with the Plexiglas blades starts softening at *370K* and because the blade wall temperature never reaches the gas temperature (*340 K*) during a test in CT2 facility, the joint remains always strong.

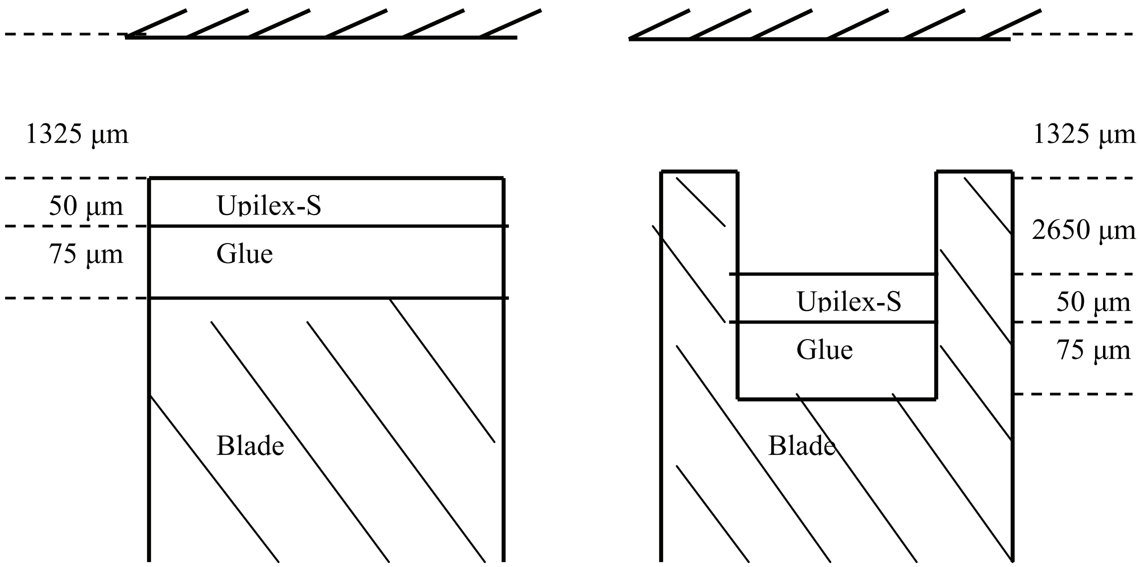

Figure 8-4: Flat and squealer tip instrumented with the two-layer gauges

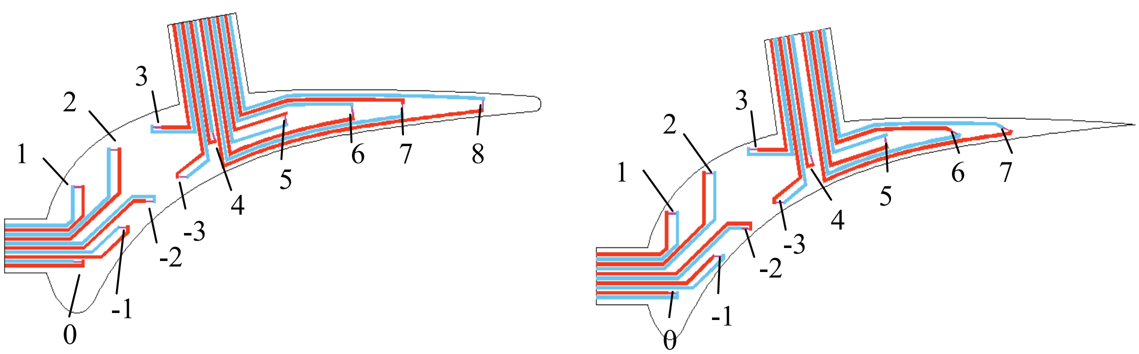

Figure 8-5: Design of the two Upilex-S sheets with the thin film resistances and their connections for the flat tip (left) and the squealer cavity (right)

The position of the sensors is exactly the same for the flat and for the squealer tip. Only due to the lack of space, the furthest downstream gauge near the trailing edge of the flat tip is not placed in the cavity of the squealer tip. Thus, the flat tip is instrumented with 12 gauges, while the squealer tip has 11 gauges. In addition, the two last gauges, the closest to the trailing edge of the squealer, are also ‘turned’ for the same reason. In any case, the gauges are always more than *3 mm* away from the tip edge or from the squealer rim to ensure the one dimensional conduction inside the blade substrate (the data reduction of the two-layer gauges is based on this one dimensional assumption, see chapter 3).

The instrumented blades are made of Plexiglas. Plexiglas is a non-conductive material from a thermal and electrical point of view; it is easily machinable and not expensive. Thus, the one dimensionality of the wall heat flux inside the blade substrate for the half second that the experiment lasts can be assured. Furthermore, the gauge connections can be carried till the bottom of the blade with no danger of short circuit with the blade. The maximum operating temperature of Plexiglas is *350K* and its softening point is *380K* and because the blade wall temperature never reaches the gas temperature (*340 K*) during a test in CT2 facility, Plexiglas does not suffer from the test campaign.

The calibration of the thermal properties of the sublayers and the thickness of the first layer of the gauges performed by Oksuz (2004) is shown in Table 8-1. (Note that the thermal product of the adhesive sheet is made to be the same as the one of Upilex-S sheet and thus, both sheets are considered as one first layer under the name of Upilex-S. This assumption was experimentally validated and shown in paragraph 3.9.3.) Another characteristic of Plexiglas is the value of its thermal product being close to the one of Upilex-S. Both layers could be then approximated to only one layer whose thermal product value is an average one of Upilex and Plexiglas. This is a fast approximation that is useful while the experimental campaign goes on, when a fast estimation of the measurements quality without the use of the data reduction program is needed. Still, the largest advantage of Plexiglas as second layer is its thermal insulation that ensures the one dimensional conduction inside the blade substrate. Although there is a high dispersion on the calibrated thermal products and especially on the thickness of the first layer, this high dispersion is not expected to generate high uncertainty on the wall heat flux calculations as the two thermal product values are close. More specific, for the case that the two thermal product values are exactly the same, the parameter of the thickness on the wall heat flux calculations becomes insignificant and the two layer case can be represented by one layer case. The analytical solution concerning the thickness value Eq. (14) for the constant wall heat flux case also shows that the closer are the two thermal product values, the bigger is the uncertainty on the thickness parameter.

	$\sqrt{(\rho c k)_1}$ Upilex-S [$J/m^2Ks^{0.5}$]	$\sqrt{(\rho c k)_2}$ Plexiglas [$J/m^2Ks^{0.5}$]	Upilex-S Thickness [μm]
Calibration value	801	739	168
Manufacturer value	692	576	125
Dispersion (20:1) [+/- %]			
	10.2	12.3	22.4

Table 8-1: Calibration of the thermal properties of the sublayers and the thickness of the first layer of the two-layer gauges

The calibrated values of Table 8-1 are compared to the values that the manufacturer gives. This comparison shows that the manufacturer values are only an estimation of the real calibrated values and that before any wall heat flux calculations, the thermal properties of the gauge substrates should be calibrated.

8.5 Measurements with the two-layer gauges on the blade tips

8.5.1 Introduction

The heat transfer measurements on the blade tips are performed in the four bladed linear cascade of the CT2 facility. This blowdown facility that operates with dry air is capable of simulating Reynolds and Mach numbers, gas/wall and gas/coolant temperature ratios of modern aero-engine HP turbines (Consigny et al., 1979). No cooling is used for the next series of measurements. By setting the above mentioned parameters, the conditions of the flow through the cascade are also set (Table 8-2).

The selected tip clearance (*1.325 mm*) is only set at the two middle blades of the cascade. The two outer blades are attached to the enwall. An additional tailboard is also adjusted to create a periodic pressure field behind the cascade (see paragraph 18.4.2).

Both blade tip geometries are subjected to the same combinations of operating conditions given in Table 8-3. The three flow parameters that vary from high to low values are the exit Reynolds number, the exit isentropic Mach number and the free stream turbulence intensity (Table 8-3). The total inlet flow temperature is selected equal to *340 K* for all the tests; This value is low enough to protect the gauges from high wall temperatures (no more than *320K*, even at the places with the highest heat transfer) during the test and high enough to give adequate accuracy on the heat transfer distributions on the blade tips.

SET parameters	1D model through the cascade	Final SET parameters
gas/wall temperature T_{01}/T_W	$T_W = T_{AMB}$ T_{01} ?	Inlet total temperature T_{01}
exit isentropic Mach number $M_{2,IS}$	$M_{2,IS} = \left[\frac{2}{\gamma - 1} \left[\left(\frac{p_2}{p_{01}} \right)^{\frac{1-\gamma}{\gamma}} - 1 \right] \right]^{0.5}$	Expansion ratio p_2/p_{01}
exit isentropic Reynolds number $Re_{2,IS}$	$Re_{2,IS} = \frac{\rho_2 u_2 C}{\mu_2} = \frac{\frac{p_2}{RT_2} M_{2,IS} \sqrt{\gamma R T_2} C}{1.485 \cdot 10^{-6} \frac{T_2^{1.5}}{110.4 + T_2}}$	Exit static pressure p_2 Inlet total pressure p_{01}

Table 8-2: Parameters that control the flow through the cascade

Conditions	Exit Reynolds number	Exit Isentropic Mach number	Turbulence intensity [%]	Inlet flow Temperature [K]
Low values	450,000	0.9	0.8	340
High values	900,000	1.1	3.8	340

Table 8-3: Operating conditions

The heat transfer distributions on the blade tips are reported under the form of the Nusselt number, Eq. (30), where T_{GAS} is the measured inlet flow temperature with a type K thermocouple, C is the blade chord (*120.5 mm*), T_W is the wall blade tip temperature measured by the gauge and Q_W is the corresponding wall heat transfer (chapter 3). The Nusselt number is calculated as a function of time and then averaged between *0.45s* and *0.55s* after the shutter opens.

Five similar tests are performed for each operating condition in order to estimate the measurement repeatability. The average Nusselt number value for each combination is given in the following graphs together with the repeatability (indicated as vertical bars at the measured point).

8.5.2 Nusselt number distribution on the flat blade tip geometry

The Nusselt number distribution on the flat blade tip for low free stream turbulence at the gauges positions is shown in Figure 8-6. The positions of the gauges are shown in Figure 8-5. On the left part of the graph (from gauge number -3 till -1), the Nusselt number of the three pressure side gauges is illustrated, while the Nusselt number of the leading edge gauge together with the three suction side gauges is demonstrated on the middle of the graph (from 0 till 3), followed by the Nusselt number of the gauges at mid-chord at the aft part of the blade (from 4 till 8). The Nusselt number is reported in a non-dimensional form for confidentiality reasons. The reference Nu_{REF} corresponds to the lowest Nusselt number value of the case described in Figure 8-6. The reduction of the wall heat fluxes was performed by Oksuz (2004).

The higher is the Reynolds number, the higher is the Nusselt number on the blade tip, at any location, when comparing two cases with the same Mach number. High Reynolds number is represented with blue and purple and low Reynolds number with red and magenta. This observation is also valid for high turbulence flat tip (Figure 8-9) and for both cases of squealer tips (low turbulence, Figure 8-11 and high turbulence, Figure 8-15). Going from low to high Reynolds number, the Nusselt number becomes almost double. In reality, the exit Reynolds number is proportional to the inlet pressure (Table 8-2) that is proportional to the inlet flow density (ρ_1).

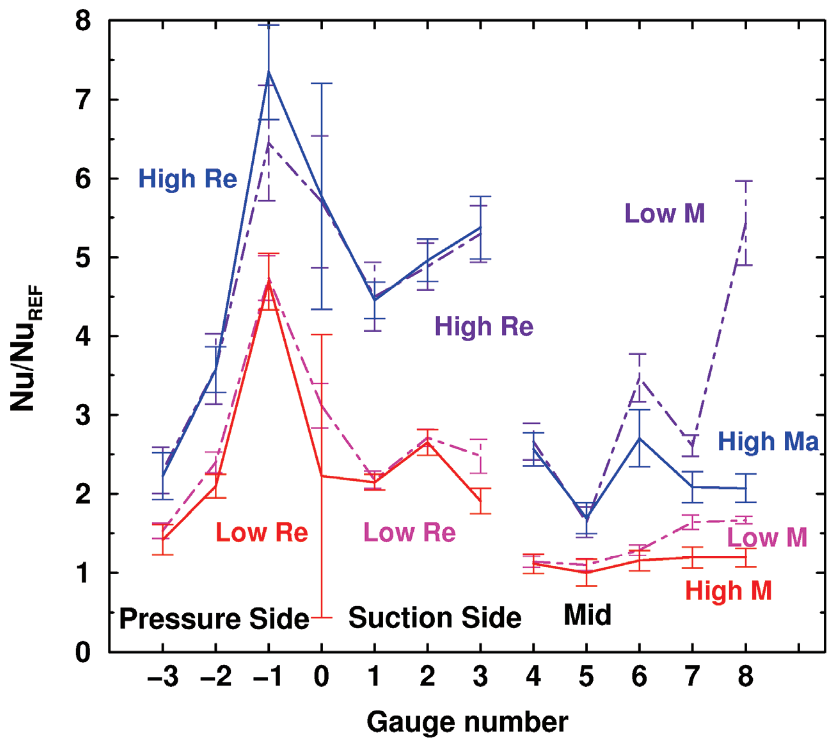

Figure 8-6: Nusselt number distribution on the flat tip for low free stream turbulence

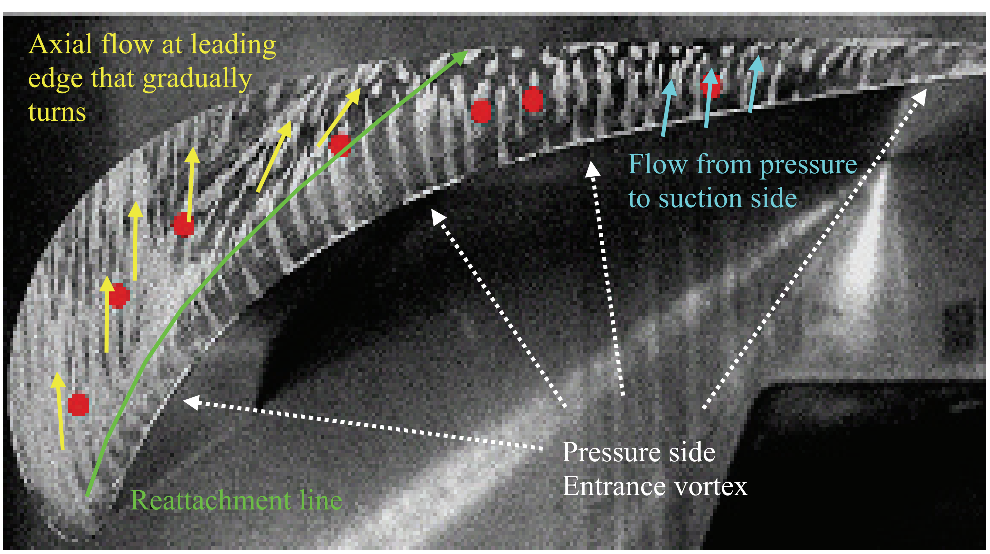

Figure 8-7: Oil flow visualization on the flat blade tip for high Reynolds, high Mach numbers (Key and Arts, 2004) - Graphical representation of the different areas of the leakage flow on the flat tip

In an attempt to combine the Nusselt number distribution on the flat blade tip with the flow pattern, additional information is needed. In Figure 8-7, the wall streamlines are visualized on the blade tip using oil dots deposited on the surface before the run (Key and Arts, 2004). The red dots on the blade correspond to pressure taps used for pressure measurements. Arrows that indicate the various flow patterns are added. A photo of the instrumented blade tip is also given in Figure 8-8. As the leakage flow enters the clearance gap, a very small entrance vortex is created along the pressure side of the blade tip (Figure 8-7). This vortex is so small and so close to the blade tip edge that no gauges can be fitted there for heat transfer measurements. An additional vortex (that produces a possible vena contracta – see 18.7.1) is created on the front part of the pressure side of the tip developing a reattachment line that starts close to the leading edge and ends up almost at 50% of the suction side of the blade tip. Behind this reattachment line, the leakage flow close to the leading edge is leaving the blade tip axially and then further downstream gradually turns towards the camber line, while it also accelerates. The leakage flow along the aft part of the tip mainly travels from the pressure side to the suction side and it is highly accelerated.

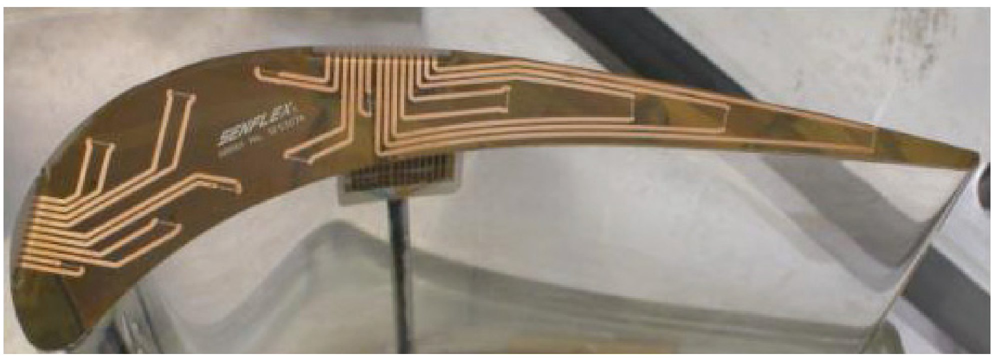

Figure 8-8: Instrumented flat blade tip with the two-layer gauges

Going back to Figure 8-6 and examining the case of high Reynolds number and high Mach number (blue line), the highest Nusselt numbers are observed on the first gauge at the pressure side (gauge number -1), while the Nusselt number drops dramatically for the next two gauges on the pressure side (gauge numbers -2 and -3). Combining the position of the gauges in Figure 8-8 with the flow pattern in Figure 8-7, the first gauge on the pressure side is located on the reattachment line and feels stagnant Nusselt number values. However, the next two gauges on the pressure side are inside the recirculation zone of the second big vortex experiencing much lower Nusselt number values.

The leading edge gauge (number 0) seems to be just downstream to the reattachment line but still close to it. The repeatability is the lowest for this gauge, mainly due to the high unsteadiness of the gauge signal during the test. It could be that this reattachment line is not well defined in this area of the blade and it moves on and out the gauge introducing high average heat transfer but still lower than the first pressure side gauge. The leading edge gauge is also tested after the CT2 tests by Oksuz (2004) in a uniform steady jet flow indicating good repeatability.

The next three gauges along the suction side of the front part of the blade tip (gauge numbers 1, 2 and 3) feel high values of heat transfer. They are behind the impingement line, in the mixing area behind the possible vena contracta, where the boundary layer could be transitional (or turbulent) due to the high mixing. However, as we go from the mid-chord to the trailing edge (gauge numbers 4, 5, 6, 7 and 8), the Nusselt number significantly falls. The high accelerated flow at the aft part of the blade could create laminar boundary layers on the blade tip 'protecting' it from higher heat transfer values.

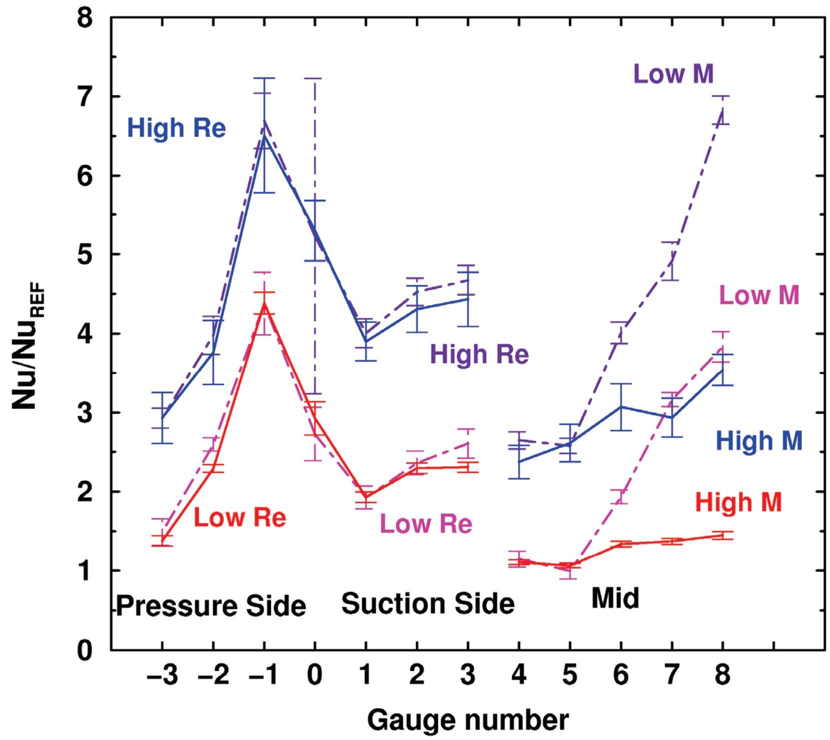

Figure 8-9: Nusselt number distribution on the flat tip for high free stream turbulence

The increasing exit Mach number increases the blade loading along the aft part of the blade. The inlet Mach number is around *0.4* for all the cases. Thus, ideally, the change of the exit Mach number does not influence the heat transfer distribution in the front part of the blade, where the blade loading does not change. According to the measured values, the average Nusselt number values of the low exit Mach number case (indicated with purple) are inside the repeatability bars of the high exit Mach number case traces (indicated with blue). However, the heat transfer increases on the aft part of the blade tip, as the Mach number decreases. In fact, the further the position of the gauges towards the trailing edge is, the higher the Nusselt number gets. Apparently, for a lower exit Mach number, the leakage flow acceleration is less strong than for a higher exit Mach number and thus the boundary layer gets from laminar (for a high exit Mach number) to transitional (for a lower exit Mach number) and could even reach turbulent features close to the trailing edge for high Reynolds numbers. The last statement is reinforced when heat transfer measurements are performed on the flat tip for higher free stream turbulence (Figure 8-9).

The change in turbulence intensity does not really influence the leakage flow field pattern at the pressure and the suction side of the front part of the blade tip. There are some small differences lower than *15%* for some gauges that could indicate a possible slight movement of the reattachment line and a faster mixing behind the vena contracta. The impressive increase of heat transfer on the aft part of the blade tip with increased turbulence intensity, especially for the cases of low exit Mach number can be well explained by the change of the boundary layer from laminar or transitional to turbulent. As the tip clearance gap is very small, measurements inside the boundary layer, which is even smaller, can not be easily performed to confirm the idea of this boundary layer change of state.

Didier et al. (2002) used four single-layer heat transfer gauges on the flat blade tip of the rotor of the one and a half stage turbine of the VKI short duration compression tube facility, CT3. The Nusselt number values of these four gauges are compared with the Nusselt number obtained from the cascade measurements in CT2 in Figure 8-10: the rotor exit Reynolds number in CT3 is

500,000 and the exit relative Mach number is *0.9*. Note that the first stator in front of the rotor operates at transonic conditions with an exit Mach number close to 1 and thus the flow at the rotor inlet is highly disturbed from the stator shock waves. The flow also gets highly unsteady as the rotor chops off the vane shock waves and wakes, while spinning at *6500 rpm*. Hence, in Figure 8-10, only the Low exit Mach number cases of the CT2 measurements are plotted that correspond to high turbulence intensity. The four gauges are positioned on the camber line of the blade tip. They are expected to be in the highly accelerated region of the leakage flow that travels from the pressure side to the suction side (Figure 8-7).

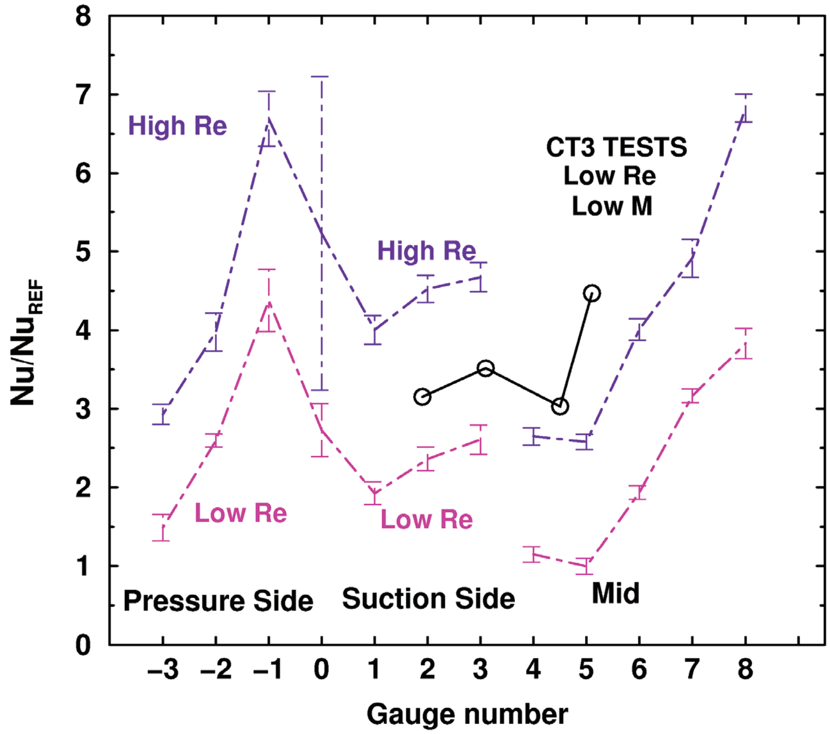

Figure 8-10: Comparison between the heat transfer measurements on the rotor tip of CT3 and the measurements on the flat tip for low Mach number and high turbulence in CT2

Although the operating conditions of the measurements in CT3 are closer to the low Reynolds number case in CT2, the CT3 measured Nusselt number values are even higher than for the high Reynolds number case in CT2. The main explanation could be based on the boundary layer status that can be transitional on the rotor tip blade (CT3) across the middle camber line compared to a more laminar state on the flat tip in CT2. Although there are only four gauges and there are no repeatability bars for the CT3 measurements, it seems that the Nusselt number increase, as we go further to the trailing edge in CT3, also starts earlier than in CT2. Both observations indicate that the free stream turbulence intensity in CT3 is higher than *4%*, higher than the cases in CT2.

Another difference between the measurements in CT2 and CT3 is the rotation of the CT3 rotor blades. According to previous work, described in appendix 18.7.6, either the rotation does not really influence the heat transfer on the blade tip (especially for bigger tip clearance gaps where the flow is mainly driven from the pressure difference between the pressure and suction side), or the rotation slightly diminishes the leakage flow and thus the heat transfer (when the viscous phenomena are stronger in the tip gap for smaller tip clearances). Note that in turbines the direction of the rotation is opposed to the direction of the leakage flow. Hence, the higher Nusselt number distribution for the gauges of CT3 should not be generated by additional rotational effects.

8.5.3 Nusselt number distribution on the squealer blade tip geometry

The Nusselt number distribution on the squealer blade tip at low free stream turbulence is shown in Figure 8-11. (The positions of the gauges are shown in Figure 8-5.) The higher the Reynolds number is, the higher the Nusselt number on the tip cavity is, at any location, when comparing two cases with the same exit Mach number, due to the increase of the inlet total pressure p_{01} (see paragraph 8.5.2).

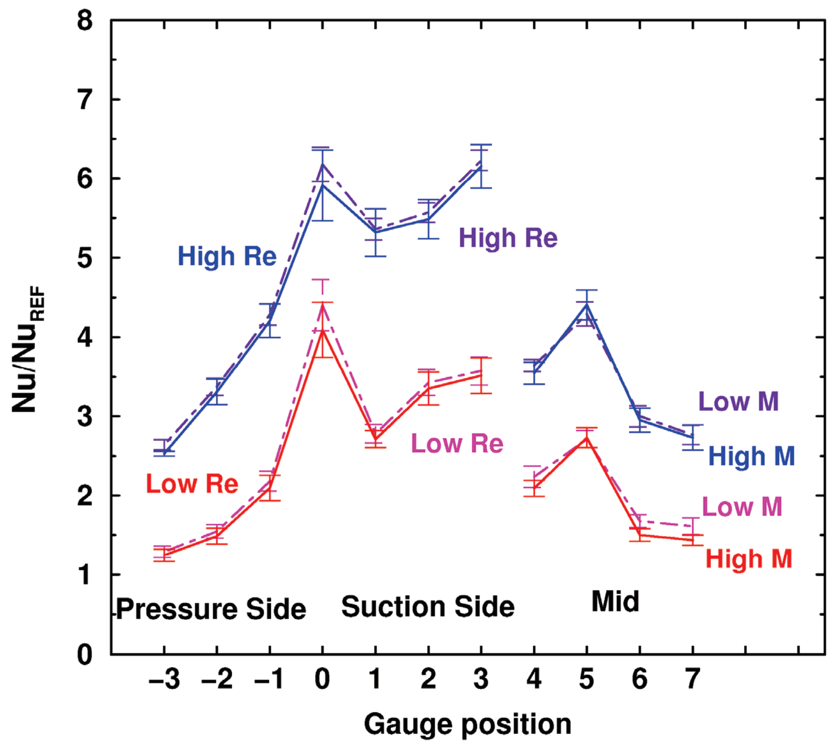

Figure 8-11: Nusselt number distribution on the squealer tip for low free stream turbulence

In an attempt to combine the Nusselt number distribution on the squealer blade tip with the flow pattern, additional information is needed. In Figure 8-12, the flow is visualized in the cavity of the blade tip using oil dots before the run (Key and Arts, 2004). Arrows that characterize the flow pattern are also added. The gauges are at the same position as for the flat tip case and a photo of the instrumented cavity of the squealer tip is also given in Figure 8-14. Only the gauge which is the closest to the trailing edge (gauge number 8) is missing for the squealer tip, due to the lack of space. The leakage flow impinges on the leading edge area of the cavity and then travels downstream in the cavity either close to the suction side or towards the pressure side rim (Figure 8-12). An additional impingement line exists along the suction side rim further downstream in the cavity. The flow in the middle of the cavity travels from suction side to pressure side, indicating that this is a region of recirculating flow. Also notice the streamwise direction of the above mentioned vortex. The flow along the pressure side rim moves toward the trailing edge with a very low momentum.

For the squealer tip and for low free stream turbulence intensity (Figure 8-11), the two gauges with the highest heat transfer are the leading edge gauge and the third suction side gauge (numbers 0, 3). The gauges are in leakage flow impingement areas, around the leading edge and across the suction side further downstream respectively. The rest of the two suction side gauges (numbers 1, 2) show a bit lower heat transfer as there are inside the area after the flow impingement at the leading edge when the flow starts traveling further downstream. The heat transfer at the pressure side (numbers -1, -2, -3) radically drops further downstream as the gauges enter the region of the low momentum fluid. The gauges on the camber line (numbers 4, 5, 6, 7) indicate very low heat transfer as they are inside the recirculating flow that travels from the suction to the pressure side of the cavity. The rather higher heat transfer on the second camber line gauge (number 5) could signify that the gauge is at the border of the recirculation zone.

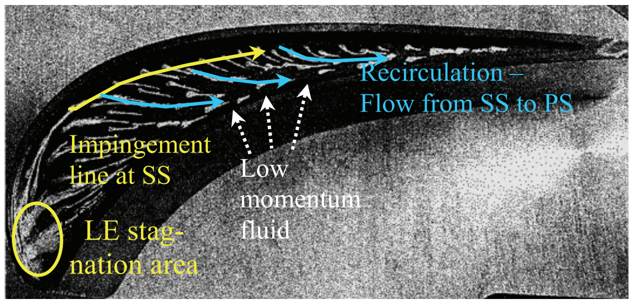

Figure 8-12: Oil flow visualization by Key and Arts (2004) - Graphical representation of the different areas of the leakage flow in the cavity of the squealer tip

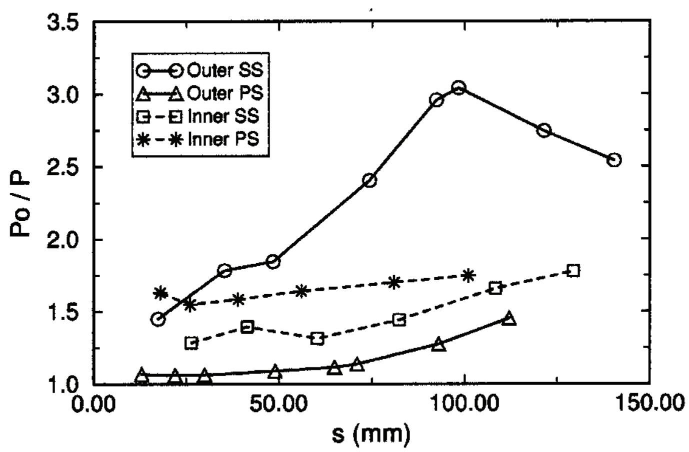

Figure 8-13: Pressure ratios inside and outside the cavity at 97.3% for the squealer tip for high Reynolds and high Mach numbers (Key and Arts, 2004)

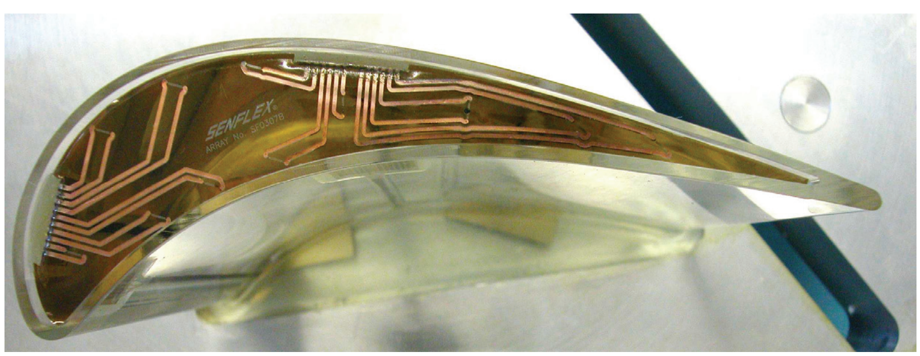

Figure 8-14: Instrumented cavity of the squealer tip with the two-layer gauges

The influence of the Mach number on the heat transfer distribution inside the squealer can be considered insignificant. All the repeatability bars of the measurements at low Mach number intersect the repeatability bars at high Mach number for the same Reynolds number. The front part of the tip (pressure and suction side) is not influenced, because there is no change of the loading at the front part with the exit Mach number. In addition, it seems that the inverse loading inside the cavity of the tip is not influenced from the outside loading on the blade pressure and suction side surfaces. This inverse loading is demonstrated in Figure 8-13 as a function of the curvilinear abscissa S (defined in Figure 4-5).

With increase free stream turbulence (Figure 8-15), the flow pattern inside the cavity of the squealer blade tip does not really change. The differences of the distribution of the Nusselt number between low and high turbulence are below *10%*, except for the second camber line gauge (number 5) that shows lower Nusselt number for higher turbulence. It could be that the different regions that define the leakage flow in the cavity slightly move with increased turbulence intensity and slightly change the local measured Nusselt number on the gauges surface.

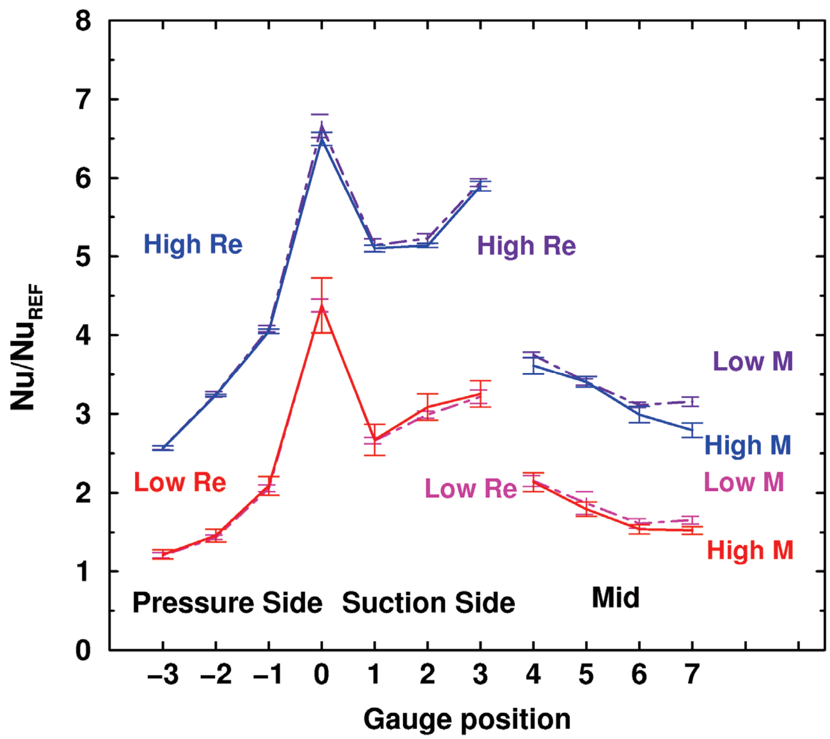

Figure 8-15: Nusselt number distribution on the squealer tip for high free stream turbulence

The comparison of the Nusselt number results between the flat tip and the squealer tip are shown in Figure 8-16, for the cases of low Mach number and high free stream turbulence intensity. The high increase of the Nusselt number on the aft part of the flat tip is avoided with the squealer tip geometry. Thus, by only changing the tip geometry from flat to squealer, the aft part of the tip gets more protected against the hot gases. However, high heat transfer rates still exist on the front part of the squealer tip and could eventually been decreased by a suitable cooling system at this area.

In addition, the Nusselt number uncertainty for the squealer measurements seems to be much lower than the one for the flat tip case. Apparently, the flow pattern on the squealer blade tip is less unsteady than the one with a flat tip. This last statement has to be reinforced with more studies on unsteady measurements. Also, the effect of the rotation and the flow distortion on the blade tip heat transfer because of the vane in front of the rotor should be the next step of this work.

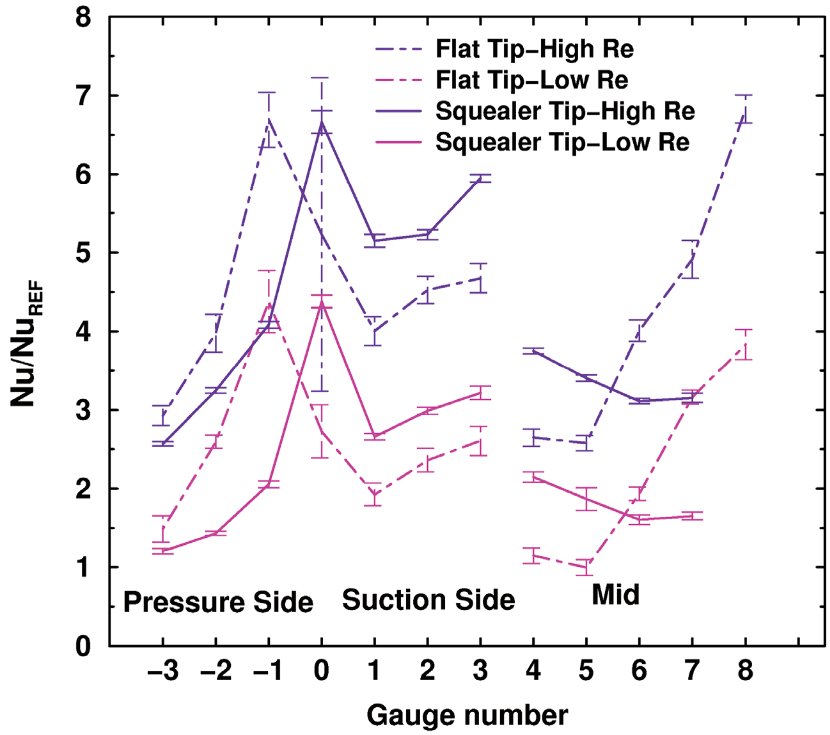

Figure 8-16: Comparison between the flat tip and the squealer tip for low Mach number and high turbulence

8.5.4 Comparisons

The flow visualization and the pressure measurements on both tip configurations of the previous work were the first necessary step to establish the tip leakage flow development. The complete understanding of the flow features on the flat and the squealer tip for different operating conditions is succeeded by the heat transfer measurements. The contribution of the two-layer gauges on this successful work has to be emphasized once more. The levels and the gradients of the Nusselt number distribution along the tips not only quantify the heat transfer at the tip areas where the flow reattaches and impinges, but also reveal new characteristics of the boundary layer development along the blade tip.

The heat transfer results of both blade tip configurations are also compared to numerical results for the case of high Reynolds number and low exit Mach number (Arts et al., 2005, where the details about the numerical method and the discretization are described). Experimental and numerical works predict the same trends, gradients and levels of Nusselt number. The only difference is observed at the suction side area of the squealer cavity; it is attributed to the poor numerical prediction of the recirculation in the squealer cavity along the suction side.

8.6 References

Ameri A.A., 2004, *'Numerical simulation of flow and heat transfer in the tip region of turbine blades'*, Turbine blade tip design and tip clearance treatment, VKI LS 2004-02

Arts T., Ginibre P., Oksuz O., Iliopoulou V., Key N., 2005, *'Comparison of turbine tip leakage aero thermal flows for flat tip and squealer'*, Proc. 6th European Conference on Turbomachinery Fluid Dynamics and Thermodynamics, Lille, France

Booth T.C., 1985, *'Importance of tip clearance flows in turbine design'*, Tip Clearance effects in Axial Turbomachines, VKI LS 1985-05

Boyle R.J., Haas J.E., Katsanis T., 1984, *'Comparison between measured turbine stage performance and the predicted performance using quasi-3D flow and boundary layer analysis'*, NASA TM-83640

Consigny H., Chan C.K., Richards B.E., 1979, *'The effect of pressure gradient and external turbulence on heat transfer to a cold flat plate'*, VKI TN 128

Glezer B., 2004, *'Thermal-mechanical design factors affecting turbine blade tip clearance'*, Turbine blade tip design and tip clearance treatment, VKI LS 2004-02

Key N.L., Arts T., 2004, *'Comparison of turbine tip leakage flow for flat tip and squealer tip geometries at high-speed conditions'*, ASME GT2004-53979, Vienna, Austria

Oksuz O., 2004, *'Aerothermal investigation of turbine tip gap flows'*, VKI PR 2004-13